REPORT NO.
UCB/SEMM-96/02

**STRUCTURAL ENGINEERING
MECHANICS AND MATERIALS**

A SYSTEMATIC CONSTRUCTION OF B-BAR FUNCTIONS FOR LINEAR AND NON-LINEAR MIXED-ENHANCED FINITE ELEMENTS

BY

R. PILTNER and R.L. TAYLOR

DECEMBER 1996

**DEPARTMENT OF CIVIL AND
ENVIRONMENTAL ENGINEERING
UNIVERSITY OF CALIFORNIA
BERKELEY, CALIFORNIA**

A SYSTEMATIC CONSTRUCTION OF B-BAR FUNCTIONS FOR LINEAR AND NON-LINEAR MIXED-ENHANCED FINITE ELEMENTS

R. PILTNER

Department of Engineering Mechanics, 229 Bancroft Hall,
University of Nebraska-Lincoln, Lincoln, NE 68588-0347, U.S.A.

R.L. TAYLOR

Department of Civil Engineering, SEMM, University of California at Berkeley,
Berkeley, CA 94720, U.S.A.

Summary

In a previous paper [1] a modified Hu-Washizu variational formulation has been used to derive an accurate four node plane strain/stress finite element denoted QE2. For the mixed element QE2 two enhanced strain terms are used and the assumed stresses satisfy the equilibrium equations *a priori* for the linear elastic case. In this paper an alternative approach is discussed. The new formulation leads to the same accuracy for linear elastic problems as the QE2 element; however it turns out to be more efficient in numerical simulations, especially for large deformation problems. Using orthogonal stress and strain functions we derive $\bar{\mathbf{B}}$ functions which avoid numerical inversion of matrices. The $\bar{\mathbf{B}}$-strain matrix is sparse and has the same structure as the strain matrix **B** obtained from a compatible displacement field. The implementation of the derived mixed element is basically the same as the one for a compatible displacement element. The only difference is that we have to compute a $\bar{\mathbf{B}}$-strain matrix instead of the standard B-matrix. Accordingly, existing subroutines for a compatible displacement element can be easily changed to obtain the mixed-enhanced finite element which yields a higher accuracy than the Q4 and QM6 elements.

1. Introduction

Several methods have been developed to improve the performance of the standard four-node compatible displacement element which yields poor results for problems with bending and, for plane strain problems, at the nearly incompressible limit. Among the improvements we like to cite the following methods:

i) Selected reduced integration [2] and the so called B-bar method [3] of Hughes.

ii) The QM6-element of Taylor/Beresford/Wilson [4] who used four incompatible quadratic

displacement functions to calculate an approximated displacement gradient.

iii) The method of "enhanced strains" introduced by Simo and Rifai [5]. Simo and Rifai also demonstrated that the QM6 element can be viewed as an enhanced strain element with four enhanced strain terms.

iv) The hybrid stress elements of Pian and Sumihara [6] and Yuan/Huang/Pian [7].

v) The mixed finite element QE2 of Piltner and Taylor [1] using a modified Hu-Washizu variational formulation with bilinear displacement interpolations, seven strain and stress terms in cartesian coordinates, and two enhanced strain modes.

The enhanced strain concept became quite popular in recent years and has been used for both linear and non-linear problems by several researchers, e.g. Simo/Armero [8], Simo/Armero/Taylor [9], Andelfinger/Ramm [10], Crisfield/Moita/Jelenic/Lyons [11], Freischläger/Schweizerhof [12], Glaser/Armero [13, 14], Korelc/Wriggers [15, 16], Nagtegaal/Fox [17], Roehl/Ramm [18], de Sausa Neto/Peric/Huang/Owen [19], Wriggers/Reese [20].

In reference [1], the stress functions for the QE2 element were chosen such that the homogeneous equilibrium equations are satisfied *a priori*. Therefore the linear version of the QE2 element can also be considered as a Trefftz-type element (e.g. [21-26]). For the QE2 element a matrix $\mathbf{H}$ has to be computed and inverted. The matrix $\mathbf{H}$ has the following block diagonal structure:

$$\mathbf{H} = \begin{bmatrix} \mathbf{H}_{11} & \mathbf{0} \\ \mathbf{0} & \mathbf{H}_{22} \end{bmatrix} \tag{1}$$

where $\mathbf{H}_{11}$ is a 3x3 diagonal matrix. So with the assumed stresses of reference [1] we are left at the element level to invert the 4x4 symmetric sub-matrix $\mathbf{H}_{22}$. In this paper we consider a method to avoid numerical inversion (except the one needed for the static condensation of the unknowns associated to the enhanced strain functions).

In addition to the improvement in efficiency of the mixed four-node finite element we address the subject of non-physical instabilities of non-linear versions of enhanced finite elements [8, 9] which have been observed by Wriggers and Reese [20] and discussed by Crisfield et al. [11] and De Sousa Neto et al. [19].

A mixed finite element with four enhanced strain terms has been tested in a series of numerical examples. The element is denoted $\bar{\mathrm{B}}$–QE4. In several numerical tests for linear problems it is shown that the elements $\bar{\mathrm{B}}$–QE4 and QE2 give identical results. The possibility of coding the $\bar{\mathrm{B}}$–QE4 element like a displacement element and its excellent performance make it attractive for non-linear applications.

2. Finite element formulation for the linear elastic case

As in reference [1] we use the following modified Hu-Washizu variational formulation:

$$\Pi(\mathbf{u}, \boldsymbol{\varepsilon}^i, \boldsymbol{\varepsilon}, \boldsymbol{\sigma}) = \int_V \frac{1}{2}\boldsymbol{\varepsilon}^T \mathbf{E}\boldsymbol{\varepsilon}\, dV - \int_V \mathbf{u}^T \bar{\mathbf{f}}\, dV - \int_S \mathbf{u}^T \bar{\mathbf{T}}\, dS - \int_V \boldsymbol{\sigma}^T (\boldsymbol{\varepsilon} - \mathbf{D}\mathbf{u} - \boldsymbol{\varepsilon}^i)\, dV \tag{2}$$

where $\boldsymbol{\varepsilon}^i$ is the enhanced strain field satisfying an orthogonality condition with respect to properly chosen reference stresses. Details about the choice of enhanced strain terms are given in reference [1].

Carrying out the variation in (2) we obtain the following equations:

$$-\int_V \delta\boldsymbol{\sigma}^T \left[\boldsymbol{\varepsilon} - \mathbf{D}\mathbf{u} - \boldsymbol{\varepsilon}^i\right] dV = 0 \tag{3}$$

$$\int_V \delta\boldsymbol{\varepsilon}^T \left[\mathbf{E}\boldsymbol{\varepsilon} - \boldsymbol{\sigma}\right] dV = 0 \tag{4}$$

$$\int_V \delta(\mathbf{D}\mathbf{u})^T \boldsymbol{\sigma}\, dV = \int_V \delta\mathbf{u}^T \bar{\mathbf{f}}\, dV + \int_S \delta\mathbf{u}^T \bar{\mathbf{T}}\, dS \tag{5}$$

$$\int_V (\delta\boldsymbol{\varepsilon}^i)^T \boldsymbol{\sigma}\, dV = 0 \tag{6}$$

The displacement, strain and stress fields are chosen in the following form:

$$\begin{aligned} \mathbf{u} &= \mathbf{N}\mathbf{q} \\ \boldsymbol{\varepsilon} &= \mathbf{S}\boldsymbol{\alpha} \\ \boldsymbol{\sigma} &= \mathbf{S}\boldsymbol{\beta} \\ \boldsymbol{\varepsilon}^i &= \mathbf{B}^i\boldsymbol{\lambda}. \end{aligned} \tag{7}$$

where $\mathbf{N} = \mathbf{N}(\xi,\eta)$ is the matrix of compatible shape functions and $\mathbf{q}$ contains the nodal displacements of the finite element. The vectors $\boldsymbol{\alpha}, \boldsymbol{\beta}, \boldsymbol{\lambda}$ are strain, stress and enhanced strain parameters, respectively. The strain field obtained from the compatible displacement field $\mathbf{u}$ can be written as

$$\mathbf{D}\mathbf{u} = \mathbf{B}\mathbf{q} \tag{8}$$

where $\mathbf{D}$ is a linear differential operator matrix. The discretization of equations (3)-(6) with arbitrary variations $\delta\boldsymbol{\beta}$, $\delta\boldsymbol{\alpha}$, $\delta\mathbf{q}$ and $\delta\boldsymbol{\lambda}$ leads to the following system of equations at the element level:

$$\begin{bmatrix} 0 & -\mathbf{H} & \mathbf{L} & \mathbf{L}^i \\ -\mathbf{H} & \mathbf{H}_T & 0 & 0 \\ \mathbf{L}^T & 0 & 0 & 0 \\ \mathbf{L}^{iT} & 0 & 0 & 0 \end{bmatrix} \begin{bmatrix} \boldsymbol{\beta} \\ \boldsymbol{\alpha} \\ \mathbf{q} \\ \boldsymbol{\lambda} \end{bmatrix} = \begin{bmatrix} 0 \\ 0 \\ \mathbf{f}_{ext} \\ 0 \end{bmatrix} \tag{9}$$

where

$$\mathbf{H} = \int_V \mathbf{S}^T\mathbf{S}\, dV$$

$$\mathbf{L} = \int_V \mathbf{S}^T\mathbf{B}\, dV$$

$$\mathbf{L}^i = \int_V \mathbf{S}^T \mathbf{B}^i \, dV \tag{10}$$

$$\mathbf{H}_T = \int_V \mathbf{S}^T \mathbf{E} \mathbf{S} \, dV$$

$$\mathbf{f}_{ext} = \int_V \mathbf{N}^T \bar{\mathbf{f}} \, dV + \int_S \mathbf{N}^T \bar{\mathbf{T}} \, dS$$

From the first two equations of (9) we obtain the strain and stress parameters as

$$\alpha = \mathbf{H}^{-1}\mathbf{L}\mathbf{q} + \mathbf{H}^{-1}\mathbf{L}^i\lambda \tag{11}$$

$$\beta = \mathbf{H}^{-1}\mathbf{H}_T\alpha = \mathbf{H}^{-1}\mathbf{H}_T\mathbf{H}^{-1}\mathbf{L}\mathbf{q} + \mathbf{H}^{-1}\mathbf{H}_T\mathbf{H}^{-1}\mathbf{L}^i\lambda. \tag{12}$$

Substitution of (11) and (12) into (9) gives us the following system of equations:

$$\begin{bmatrix} \mathbf{L}^T\mathbf{H}^{-1}\mathbf{H}_T\mathbf{H}^{-1}\mathbf{L} & \mathbf{L}^T\mathbf{H}^{-1}\mathbf{H}_T\mathbf{H}^{-1}\mathbf{L}^i \\ \mathbf{L}^{iT}\mathbf{H}^{-1}\mathbf{H}_T\mathbf{H}^{-1}\mathbf{L} & \mathbf{L}^{iT}\mathbf{H}^{-1}\mathbf{H}_T\mathbf{H}^{-1}\mathbf{L}^i \end{bmatrix} \begin{bmatrix} \mathbf{q} \\ \lambda \end{bmatrix} = \begin{bmatrix} \mathbf{f}_{ext} \\ \mathbf{0} \end{bmatrix} \tag{13}$$

or

$$\begin{bmatrix} \mathbf{K} & \Gamma^T \\ \Gamma & \mathbf{Q} \end{bmatrix} \begin{bmatrix} \mathbf{q} \\ \lambda \end{bmatrix} = \begin{bmatrix} \mathbf{f}_{ext} \\ \mathbf{0} \end{bmatrix} \tag{14}$$

where

$$\mathbf{K} = \mathbf{L}^T\mathbf{H}^{-1}\mathbf{H}_T\mathbf{H}^{-1}\mathbf{L}$$

$$\Gamma = \mathbf{L}^{iT}\mathbf{H}^{-1}\mathbf{H}_T\mathbf{H}^{-1}\mathbf{L} \tag{15}$$

$$\mathbf{Q} = \mathbf{L}^{iT}\mathbf{H}^{-1}\mathbf{H}_T\mathbf{H}^{-1}\mathbf{L}^i.$$

Using a static condensation process with respect to the enhanced strain parameters λ we finally get the element stiffness matrix in the form

$$\mathbf{k} = \mathbf{K} - \Gamma^T\mathbf{Q}^{-1}\Gamma \tag{16}$$

In order to avoid calculating the matrices $\mathbf{L}$, $\mathbf{H}$, $\mathbf{H}_T$, $\mathbf{L}$, $\mathbf{L}^i$ as well as performing the numerical inversion of $\mathbf{H}$ and matrix multiplications in (15), we seek a more efficient way to compute the matrices $\mathbf{K}$, Γ and $\mathbf{Q}$. The key for an efficient implementation of the mixed finite element is to exploit the structure of the matrices $\mathbf{H}$, $\mathbf{L}$, $\mathbf{L}^i$ for a proper choice of stress and strain functions collected in the matrix $\mathbf{S}$.

In order to achieve high accuracy with our finite element we choose the strain and stress functions in cartesian coordinates. This choice is motivated by the good numerical results of the element QE2 and the Trefftz-type finite elements from references [21-26] for which stresses in cartesian coordinates have been chosen such that the equilibrium equations are satisfied *a priori*. The disadvantage of the set of assumed stresses for element QE2 (see equ. (77) in [1]) is that the matrix of assumed stresses is full and did not lead to a diagonal matrix $\mathbf{H}$. In reference [1] a block diagonal matrix with one 3x3 diagonal sub-matrix and a 4x4 fully populated sub-matrix was constructed.

For the present element we do not require that the assumed stresses satisfy equilibrium at the element level *a priori* for arbitrary stress parameters β, as was the case in reference [1]. Instead we require only that the stresses can satisfy the equilibrium equations for proper relations between the stress parameters β_j collected in the vector $\boldsymbol{\beta}$. This implies that we now need more stress terms than in reference [1], where seven stress terms have been used.

For the mixed two dimensional element we can assume the stress field in the form

$$\sigma = \begin{bmatrix} \sigma_{xx} \\ \sigma_{yy} \\ \tau_{xy} \end{bmatrix} = \begin{bmatrix} S_1 & S_2 & S_3 & 0 & 0 & 0 & 0 & 0 & 0 \\ 0 & 0 & 0 & S_1 & S_2 & S_3 & 0 & 0 & 0 \\ 0 & 0 & 0 & 0 & 0 & 0 & S_1 & S_2 & S_3 \end{bmatrix} \begin{bmatrix} \\ \beta \\ \\ \end{bmatrix} = S\,\beta \tag{17}$$

where the S_j are linearly independent functions in cartesian coordinates. For the strain field we use the same matrix **S** as for the stress trial field. Unlike the assumed stresses for element QE2 (see equ. (77) in reference [1]) the assumed stress components of (17) are not coupled. The resulting matrix **H** has the following block diagonal structure:

$$\mathbf{H} = \begin{bmatrix} \hat{\mathbf{H}} & 0 & 0 \\ 0 & \hat{\mathbf{H}} & 0 \\ 0 & 0 & \hat{\mathbf{H}} \end{bmatrix} \tag{18}$$

If our linearly independent trial functions S_j (j = 1, 2, 3) do not satisfy the orthogonality condition

$$\int_V S_i^T S_j \, dV \begin{cases} = 0 & \text{for } i \neq j \\ \neq 0 & \text{for } i = j \end{cases} \tag{19}$$

we will get a fully populated 3x3 matrix $\hat{\mathbf{H}}$. Since the matrix **H** has to be inverted it is better to orthogonalize a set of linearly independent functions so that $\hat{\mathbf{H}}$ and therefore **H** become diagonal.

Possible choices for our initial (non-orthogonal) set of linearly independent trial functions S_j are

$$S_1 = 1, \qquad S_2 = \bar{x}, \qquad S_3 = \bar{y}, \tag{20}$$

and

$$S_1 = 1, \qquad S_2 = \bar{\xi}, \qquad S_3 = \bar{\eta}, \tag{21}$$

where $\bar{x}$, $\bar{y}$ are cartesian coordinates with origin at the center of the quadrilateral finite element. The coordinates $\bar{\xi}$, $\bar{\eta}$ are obtained as a linear combination of the cartesian coordinates $\bar{x}$, $\bar{y}$ from the relationship

$$\begin{bmatrix} \bar{\xi} \\ \bar{\eta} \end{bmatrix} = \frac{1}{J_0} \begin{bmatrix} b_2 & -a_2 \\ -b_1 & a_1 \end{bmatrix} \begin{bmatrix} \bar{x} \\ \bar{y} \end{bmatrix} \tag{22}$$

The relationship between the global cartesian coordinates x, y and the local coordinates $\bar{x}$, $\bar{y}$ is given as

$$\bar{x} = x - a_0\,, \qquad \bar{y} = y - b_0 \tag{23}$$

where

$$a_0 = \frac{1}{4}(x_1 + x_2 + x_3 + x_4), \qquad b_0 = \frac{1}{4}(y_1 + y_2 + y_3 + y_4), \tag{24}$$

The coefficients of the linear mapping (22) are given as

$$\begin{aligned} a_1 &= \frac{1}{4}(-x_1 + x_2 + x_3 - x_4), \qquad b_1 = \frac{1}{4}(-y_1 + y_2 + y_3 - y_4), \\ a_2 &= \frac{1}{4}(-x_1 - x_2 + x_3 + x_4), \qquad b_2 = \frac{1}{4}(-y_1 - y_2 + y_3 + y_4), \\ J_0 &= a_1 b_2 - a_2 b_1 \end{aligned} \tag{25}$$

Finally we can express the local element coordinates $\bar{x}$, $\bar{y}$ and $\bar{\xi}$, $\bar{\eta}$ through the natural element coordinates ξ, η via

$$\begin{aligned} \bar{x} &= a_1\xi + a_2\eta + a_3\xi\eta \\ \bar{y} &= b_1\xi + b_2\eta + b_3\xi\eta \end{aligned} \tag{26}$$

and

$$\begin{aligned} \bar{\xi} &= \xi + \frac{J_2}{J_0}\xi\eta \\ \bar{\eta} &= \eta + \frac{J_1}{J_0}\xi\eta \end{aligned} \tag{27}$$

where

$$a_3 = \frac{1}{4}(x_1 - x_2 + x_3 - x_4), \qquad b_3 = \frac{1}{4}(y_1 - y_2 + y_3 - y_4), \tag{28}$$

and

$$\begin{aligned} J_1 &= a_1 b_3 - b_1 a_3 \\ J_2 &= a_3 b_2 - a_2 b_3 \end{aligned} \tag{29}$$

Since the expressions (27) are simpler than (26) we choose $[\,\hat{S}_1 = 1, \quad \hat{S}_2 = \bar{\xi}, \quad \hat{S}_3 = \bar{\eta}\,]$ as initial set of linearly independent trial functions to construct an orthogonal set of linearly independent functions $[\,S_1, \quad S_2, \quad S_3]$.

This can be achieved by a Gram-Schmidt-orthogonalization process through the formula

$$S_j = \hat{S}_j - \sum_{k=1}^{j-1} \frac{\int_V \hat{S}_j S_k \, dV}{\int_V S_k S_k \, dV} \; S_k \tag{30}$$

The resulting set of orthogonal functions is

$$\begin{aligned} S_1 &= 1 \\ S_2 &= \bar{\xi} - \frac{J_1}{3J_0} \end{aligned} \tag{31}$$

$$S_3 = \bar{\eta} - \frac{J_2}{3J_0} - f\,S_2$$

where

$$f = \frac{2J_1J_2}{3J_2^2 - J_1^2 + 3J_0^2} \tag{32}$$

and $\bar{\xi}$, $\bar{\eta}$ are obtained from equation (27).

With the choice of functions [S_1, S_2, S_3] from equation (31) the entries of the matrix S for the stress and strain fields are defined.

The compatible displacement field **u** is interpolated with standard shape functions according

$$\mathbf{u} = \begin{bmatrix} u \\ v \end{bmatrix} = \sum_{i=1}^{4} \frac{1}{4}(1+\xi_i\xi)(1+\eta_i\eta) \begin{bmatrix} u_i \\ v_i \end{bmatrix} = \sum_{i=1}^{4} N_i \begin{bmatrix} u_i \\ v_i \end{bmatrix} = \mathbf{Nq} \tag{33}$$

An admissible enhanced strain field with four terms can be obtained from the incompatible displacement field

$$\mathbf{u}^i = \begin{bmatrix} N_1^{enh} & 0 & N_2^{enh} & 0 \\ 0 & N_1^{enh} & 0 & N_2^{enh} \end{bmatrix} \begin{bmatrix} \lambda_1 \\ \lambda_2 \\ \lambda_3 \\ \lambda_4 \end{bmatrix} \tag{34}$$

where

$$N_1^{enh} = 1 - \xi^2\,, \qquad N_2^{enh} = 1 - \eta^2 \tag{35}$$

Instead of using the exact gradient of the shape functions

$$\nabla N_j^{enh} = \begin{bmatrix} \frac{\partial}{\partial x} \\ \frac{\partial}{\partial y} \end{bmatrix} N_j^{enh} = \frac{1}{J(\xi,\eta)} \begin{bmatrix} y_\eta(\xi,\eta) & -y_\xi(\xi,\eta) \\ -x_\eta(\xi,\eta) & x_\xi(\xi,\eta) \end{bmatrix} \begin{bmatrix} \frac{\partial}{\partial \xi} \\ \frac{\partial}{\partial \eta} \end{bmatrix} N_j^{enh} = \mathbf{J}^{-1}(\xi,\eta) \begin{bmatrix} \frac{\partial}{\partial \xi} \\ \frac{\partial}{\partial \eta} \end{bmatrix} N_j^{enh} \tag{36}$$

the approximated gradient

$$\nabla_0 N_j^{enh} = \begin{bmatrix} \frac{\partial^0}{\partial x} \\ \frac{\partial^0}{\partial y} \end{bmatrix} N_j^{enh} = \frac{1}{J(\xi,\eta)} \begin{bmatrix} y_\eta(0,0) & -y_\xi(0,0) \\ -x_\eta(0,0) & x_\xi(0,0) \end{bmatrix} \begin{bmatrix} \frac{\partial}{\partial \xi} \\ \frac{\partial}{\partial \eta} \end{bmatrix} N_j^{enh} = \frac{J_0}{J(\xi,\eta)} \mathbf{J}_0^{-1} \begin{bmatrix} \frac{\partial}{\partial \xi} \\ \frac{\partial}{\partial \eta} \end{bmatrix} N_j^{enh} \tag{37}$$

as proposed by Taylor/Beresford/Wilson in reference [4] is used to get the following admissible enhanced strain field:

$$\boldsymbol{\varepsilon}^i = \begin{bmatrix} \varepsilon_{xx}^i \\ \varepsilon_{yy}^i \\ \gamma_{xy}^i \end{bmatrix} = \mathbf{B}^i\boldsymbol{\lambda} = \frac{2}{J(\xi,\eta)} \begin{bmatrix} -b_2\xi & 0 & b_1\eta & 0 \\ 0 & a_2\xi & 0 & -a_1\eta \\ a_2\xi & -b_2\xi & -a_1\eta & b_1\eta \end{bmatrix} \begin{bmatrix} \lambda_1 \\ \lambda_2 \\ \lambda_3 \\ \lambda_4 \end{bmatrix} \tag{38}$$

where the determinant J of the Jacobian matrix can be expressed as

$$J(\xi,\eta) = J_0 + J_1\xi + J_2\eta \tag{39}$$

With the assumed displacement, strain and stress fields, all integrals in the element formulation can be calculated exactly with 2x2 Gauss-integration since the expressions for the matrices $\mathbf{H}$, $\mathbf{H}_T$, $\mathbf{L}$, and $\mathbf{L}^i$ contain only polynomials in ξ and η. This is in contrast to the situation in the displacement element formulation where we can not get exact integral results for an arbitrary quadrilateral element shape. This is due to the factor $1/J(\xi,\eta)$ in all integrals for the stiffness matrix.

The diagonal matrix $\mathbf{H}$ is defined through the entries of the 3x3 matrix $\hat{\mathbf{H}}$. Through analytical integration we get the diagonal coefficients of the matrix $\hat{\mathbf{H}}$ as:

$$\begin{aligned}
\hat{h}_{11} &= 4J_0 \\
\hat{h}_{22} &= \frac{4}{9}J_0(3j_2^2 - j_1^2 + 3) \\
\hat{h}_{33} &= -\frac{4(3 + 2j_1^2 - j_1^4 + 2j_2^2 + 2j_1^2j_2^2 - j_2^4)}{3(3j_2^2 - j_1^2 + 3)}J_0
\end{aligned} \tag{40}$$

where $j_1 = J_1/J_0$ and $j_2 = J_2/J_0$. The strain matrices $\mathbf{B}$ and $\mathbf{B}^i$ have the structure

$$\mathbf{B} = \begin{bmatrix} N_{1,x} & 0 & N_{2,x} & 0 & N_{3,x} & 0 & N_{4,x} & 0 \\ 0 & N_{1,y} & 0 & N_{2,y} & 0 & N_{3,y} & 0 & N_{4,y} \\ N_{1,y} & N_{1,x} & N_{2,y} & N_{2,x} & N_{3,y} & N_{3,x} & N_{4,y} & N_{4,x} \end{bmatrix} \tag{41}$$

and

$$\mathbf{B}^i = \begin{bmatrix} \frac{\partial^0}{\partial x}N_1^{enh} & 0 & \frac{\partial^0}{\partial x}N_2^{enh} & 0 \\ 0 & \frac{\partial^0}{\partial y}N_1^{enh} & 0 & \frac{\partial^0}{\partial y}N_2^{enh} \\ \frac{\partial^0}{\partial y}N_1^{enh} & \frac{\partial^0}{\partial x}N_1^{enh} & \frac{\partial^0}{\partial y}N_2^{enh} & \frac{\partial^0}{\partial x}N_2^{enh} \end{bmatrix} \tag{42}$$

where $\frac{\partial^0}{\partial x}$ and $\frac{\partial^0}{\partial y}$ indicate that the derivatives of the incompatible shape functions are an approximation given by equation (37).

It is important to notice that due to the sparse structure of $\mathbf{S}$, $\mathbf{B}$ and $\mathbf{B}^i$ and the fact that these matrices have repeated entries for their coefficients the matrices $\mathbf{L}$ and $\mathbf{L}^i$ have only a few non-vanishing different coefficients. The non-vanishing coefficients are denoted by f_x^{ij}, f_y^{ij}, $f_{x,enh}^{ik}$, $f_{y,enh}^{ik}$, where (i = 1, 2, 3), (j = 1, 2, 3, 4), (k = 1, 2) and given by

$$\begin{aligned}
f_x^{ij} &= \int_V S_i(\xi,\eta)\frac{\partial}{\partial x}N_j(\xi,\eta)\,dV. \\
f_y^{ij} &= \int_V S_i(\xi,\eta)\frac{\partial}{\partial y}N_j(\xi,\eta)\,dV. \\
f_{x,enh}^{ik} &= \int_V S_i(\xi,\eta)\frac{\partial^0}{\partial x}N_k^{enh}(\xi,\eta)\,dV.
\end{aligned} \tag{43}$$

$$f_{y,enh}^{ik} = \int_V S_i(\xi,\eta)\frac{\partial^0}{\partial y}N_k^{enh}(\xi,\eta)\,dV.$$

There is no particular advantage to give analytical expressions for the results of the integrals in equations (43). The exact values for f_x^{ij}, f_y^{ij}, $f_{x,enh}^{ik}$, and $f_{y,enh}^{ik}$ can be obtained with 2x2 Gaussian integration. Having calculated the exact coefficients of the diagonal matrix $\mathbf{H}$ and the sparse matrices $\mathbf{L}$ and $\mathbf{L}^i$ we can calculate the strain parameters α from relationship (11). Now we can write the assumed strain field in the form:

$$\boldsymbol{\varepsilon} = \bar{\mathbf{B}}\mathbf{q} + \bar{\mathbf{B}}^i\boldsymbol{\lambda} \tag{44}$$

where

$$\bar{\mathbf{B}} = \begin{bmatrix} \bar{N}_x^1 & 0 & \bar{N}_x^2 & 0 & \bar{N}_x^3 & 0 & \bar{N}_x^4 & 0 \\ 0 & \bar{N}_y^1 & 0 & \bar{N}_y^2 & 0 & \bar{N}_y^3 & 0 & \bar{N}_y^4 \\ \bar{N}_y^1 & \bar{N}_x^1 & \bar{N}_y^2 & \bar{N}_x^2 & \bar{N}_y^3 & \bar{N}_x^3 & \bar{N}_y^4 & \bar{N}_x^4 \end{bmatrix} \tag{45}$$

and

$$\bar{\mathbf{B}}^i = \begin{bmatrix} \bar{N}_{x,enh}^1 & 0 & \bar{N}_{x,enh}^2 & 0 \\ 0 & \bar{N}_{y,enh}^1 & 0 & \bar{N}_{y,enh}^2 \\ \bar{N}_{y,enh}^1 & \bar{N}_{x,enh}^1 & \bar{N}_{y,enh}^2 & \bar{N}_{x,enh}^2 \end{bmatrix} \tag{46}$$

The matrices $\bar{\mathbf{B}}$, $\bar{\mathbf{B}}^i$ have the same sparse structure as the matrices $\mathbf{B}$, $\mathbf{B}^i$. Taking into account that $S_1 = 1$, the $\bar{N}$ functions can be written as

$$\begin{aligned}
\bar{N}_x^j(\xi,\eta) &= \frac{f_x^{1j}}{\hat{h}_{11}} + \frac{f_x^{2j}}{\hat{h}_{22}}S_2(\xi,\eta) + \frac{f_x^{3j}}{\hat{h}_{33}}S_3(\xi,\eta) \\
\bar{N}_y^j(\xi,\eta) &= \frac{f_y^{1j}}{\hat{h}_{11}} + \frac{f_y^{2j}}{\hat{h}_{22}}S_2(\xi,\eta) + \frac{f_y^{3j}}{\hat{h}_{33}}S_3(\xi,\eta) \\
\bar{N}_{x,enh}^k(\xi,\eta) &= \frac{f_{x,enh}^{1k}}{\hat{h}_{11}} + \frac{f_{x,enh}^{2k}}{\hat{h}_{22}}S_2(\xi,\eta) + \frac{f_{x,enh}^{3k}}{\hat{h}_{33}}S_3(\xi,\eta) \\
\bar{N}_{y,enh}^k(\xi,\eta) &= \frac{f_{y,enh}^{1k}}{\hat{h}_{11}} + \frac{f_{y,enh}^{2k}}{\hat{h}_{22}}S_2(\xi,\eta) + \frac{f_{y,enh}^{3k}}{\hat{h}_{33}}S_3(\xi,\eta)
\end{aligned} \tag{47}$$

where (j = 1, 2, 3, 4) and (k = 1, 2).

Note that the matrices $\bar{\mathbf{B}}$ and $\bar{\mathbf{B}}^i$ contain polynomials in ξ, η whereas the matrices $\mathbf{B}$ and $\mathbf{B}^i$ contain rational functions of the natural element coordinates ξ and η.

Instead of computing the matrices $\mathbf{K}$, Γ and $\mathbf{Q}$ from equations (15), which involves time consuming matrix multiplications of $\mathbf{H}$, $\mathbf{L}$, $\mathbf{L}^i$, $\mathbf{H}_T$ we can compute them faster by using the sparse strain matrices $\bar{\mathbf{B}}$ and $\bar{\mathbf{B}}^i$:

$$\mathbf{K} = = \int_V \bar{\mathbf{B}}^T\mathbf{E}\bar{\mathbf{B}}\,dV$$

$$\Gamma = = \int_V \bar{B}^{iT} E \bar{B} \, dV \tag{48}$$

$$Q = = \int_V \bar{B}^{iT} E \bar{B}^{i} \, dV$$

The external load vector involves compatible shape functions from equation (33) and is given by

$$f_{ext} = \int_V N^T \bar{f} \, dV + \int_S N^T \bar{T} \, dS \tag{49}$$

3. Formulation for large deformation of hyperelastic materials

In this section we will first use tensor notation and later switch to matrix and vector notation. For an overview on non-linear elasticity we refer to Beatty's review articles [27] and [28]. For the large deformation case we will use the first (un-symmetric) Piola-Kirchhoff stress tensor **P** which is related to the second (symmetric) Piola-Kirchhoff stress tensor **S**, the Kichhoff stresses τ and the Cauchy stresses σ through the relation

$$\mathbf{P} = \mathbf{FS} = \tau \mathbf{F}^{-T} = J \sigma \mathbf{F}^{-T}. \tag{50}$$

where **F** is the deformation gradient

$$\mathbf{F} = \frac{\partial \mathbf{x}}{\partial \mathbf{X}} = \mathbf{I} + \text{Grad } \mathbf{u}. \tag{51}$$

In this notation, **x** is the position vector in the current configuration whereas **X** denotes the position vector in the reference configuration. Using **u** as the displacement vector, the position vectors are related through the equation

$$\mathbf{x} = \mathbf{X} + \mathbf{u} \tag{52}$$

The displacement gradient with respect to the reference configuration is given for our two dimensional example by

$$\text{Grad } \mathbf{u} = \begin{bmatrix} \frac{\partial u}{\partial X} & \frac{\partial u}{\partial Y} \\ \frac{\partial v}{\partial X} & \frac{\partial v}{\partial Y} \end{bmatrix} \tag{53}$$

The relations for the symmetric Kirchhoff stress tensor τ and the Cauchy stress tensor σ are given by

$$\tau = \mathbf{P}\mathbf{F}^T = \mathbf{F}\mathbf{S}\mathbf{F}^T$$

$$\sigma = \frac{1}{J}\tau \tag{54}$$

Here we want to consider the case of a hyperelastic material which is characterized through a frame invariant stored energy function $W(\mathbf{X},\mathbf{F})$. For objectivity the strain energy function must satisfy the relation

$$W(\mathbf{X}, \mathbf{QF}) = W(\mathbf{X}, \mathbf{F}) \tag{55}$$

for all proper orthogonal $\mathbf{Q}$. For a hyperelastic material the un-symmetric Piola-Kirchhoff stress tensor is given by

$$\mathbf{P} = \frac{\partial W}{\partial \mathbf{F}} \tag{56}$$

In the finite element implementation we will make use of the incremental relation

$$\Delta \mathbf{P} = \mathbf{A} : \Delta \mathbf{F} \tag{57}$$

or in index notation

$$\Delta P_{iJ} = A_{iJkL} \Delta F_{kL} \tag{58}$$

The fourth order tensor $\mathbf{A}$, which is called the first elasticity tensor, is given through

$$\mathbf{A} = \frac{\partial^2 W}{\partial \mathbf{F} \partial \mathbf{F}} \quad \text{or} \quad A_{iJkL} = \frac{\partial^2 W}{\partial F_{iJ} \partial F_{kL}} \tag{59}$$

Using an assumed displacement gradient $\mathbf{G_u}$ and an enhanced displacement gradient $\text{Grad}_0\, \mathbf{u}_{enh}$ in the reference configuration the modified Hu-Washizu formulation for large deformations can be given as

$$\begin{aligned} \delta\Pi = & \int_V \text{Grad}\, \delta\mathbf{u} : \mathbf{P}\, dV + \delta\Pi_{ext.} \\ & - \int_V \delta\mathbf{P} : \left[\mathbf{G_u} - \text{Grad}\, \mathbf{u} - \text{Grad}_0\, \mathbf{u}_{enh} \right] dV \\ & + \int_V \delta\mathbf{G_u} : \left[\frac{\partial W}{\partial \mathbf{F}} \Big|_{(\mathbf{F} = \mathbf{I} + \mathbf{G_u})} - \mathbf{P} \right] dV \\ & + \int_V \delta[\text{Grad}_0 \mathbf{u}_{enh}] : \mathbf{P}\, dV \end{aligned} \tag{60}$$

where $\delta\mathbf{F} = \text{Grad}\, \delta\mathbf{u}$ and

$$\mathbf{G_u} = \begin{bmatrix} \tilde{u}_X & \tilde{u}_Y \\ \tilde{v}_X & \tilde{v}_Y \end{bmatrix}, \qquad \text{Grad}_0\, \mathbf{u}_{enh} = \begin{bmatrix} \dfrac{\partial^0 u_{enh}}{\partial X} & \dfrac{\partial^0 u_{enh}}{\partial Y} \\ \dfrac{\partial^0 v_{enh}}{\partial X} & \dfrac{\partial^0 v_{enh}}{\partial Y} \end{bmatrix} \tag{61}$$

$$\mathbf{P} = \begin{bmatrix} P_{11} & P_{12} \\ P_{21} & P_{22} \end{bmatrix} \tag{62}$$

have been used. For a discretization of (60) we switch to matrix and vector notation. Using the vectors

$$\begin{aligned} \mathbf{P}^T &= [P_{11},\ P_{22},\ P_{12},\ P_{21}] \\ \nabla\mathbf{u}^T &= [u_X,\ v_Y,\ u_Y,\ v_X] \\ \mathbf{g}_\mathbf{u}^T &= [\tilde{u}_X,\ \tilde{v}_Y,\ \tilde{u}_Y,\ \tilde{v}_X] \\ \nabla_0 \mathbf{u}_{enh}^T &= [u_X^{enh},\ v_Y^{enh},\ u_Y^{enh},\ v_X^{enh}] \end{aligned} \tag{63}$$

The variational formulation can be expressed as:

$$\delta\Pi = \int_V \nabla\,\delta\mathbf{u}^T\,\mathbf{P}\,dV + \delta\Pi_{ext.} - \int_V \delta\mathbf{P}^T\left[\mathbf{g}_u^T - \nabla\,\mathbf{u} - \nabla_0\,\mathbf{u}_{enh}\right] dV + \int_V \delta\mathbf{g}_u\left[\tilde{\mathbf{P}}(\mathbf{g}_u) - \mathbf{P}\right] dV + \int_V \delta\nabla\mathbf{u}_{enh}^T\,\mathbf{P}\,dV \tag{64}$$

where $\tilde{\mathbf{P}}$ denotes the vector of Piola-Kirchhoff stresses vector obtained from $\partial W/\partial \mathbf{F}$ by using the assumed displacement gradient $\mathbf{G_u}$. An increment for the Piola-Kirchhoff stress depending on an increment $\Delta\mathbf{g_u}$ can be calculated from

$$\Delta\tilde{\mathbf{P}} = \mathbf{A_T}\,\Delta\mathbf{g_u} \tag{65}$$

An expression for the tangent moduli $\mathbf{A_T}$ for one of the chosen constitutive models is given in Section 4.

For the increments of stresses and displacement gradients we assume the functions

$$\begin{aligned}\Delta\mathbf{P} &= \mathbf{S}\,\Delta\boldsymbol{\beta}\\ \Delta\mathbf{g_u} &= \mathbf{S}\,\Delta\boldsymbol{\alpha}\\ \nabla(\Delta\mathbf{u}) &= \mathbf{B}\,\Delta\mathbf{q}\\ \nabla_0(\Delta\mathbf{u}_{enh}) &= \mathbf{B}^{enh}\,\Delta\boldsymbol{\lambda}\end{aligned} \tag{66}$$

where

$$\mathbf{S} = \begin{bmatrix} S_1 & S_2 & S_3 & 0 & 0 & 0 & 0 & 0 & 0 & 0 & 0 & 0\\ 0 & 0 & 0 & S_1 & S_2 & S_3 & 0 & 0 & 0 & 0 & 0 & 0\\ 0 & 0 & 0 & 0 & 0 & 0 & S_1 & S_2 & S_3 & 0 & 0 & 0\\ 0 & 0 & 0 & 0 & 0 & 0 & 0 & 0 & 0 & S_1 & S_2 & S_3 \end{bmatrix} \tag{67}$$

$$\mathbf{B} = \begin{bmatrix} N_{1,X} & 0 & N_{2,X} & 0 & N_{3,X} & 0 & N_{4,X} & 0\\ 0 & N_{1,Y} & 0 & N_{2,Y} & 0 & N_{3,Y} & 0 & N_{4,Y}\\ N_{1,Y} & 0 & N_{2,Y} & 0 & N_{3,Y} & 0 & N_{4,Y} & 0\\ 0 & N_{1,X} & 0 & N_{2,X} & 0 & N_{3,X} & 0 & N_{4,X} \end{bmatrix} \tag{68}$$

$\mathbf{B}^{enh}$ is the matrix for the enhanced displacement gradient. Unfortunately, for the large deformation case we cannot use a sparse matrix for the enhanced displacement gradient. Using a sparse matrix $\mathbf{B}^{enh}$ yields an element which is not frame invariant. The following matrix $\mathbf{B}^{enh}$ has been chosen for the proposed enhanced element:

$$\underline{\mathbf{B}}^{enh} = \frac{1}{J(\xi,\eta)}\begin{bmatrix} b_2^2\xi & -b_1b_2\xi & -b_1b_2\eta & b_1^2\eta\\ a_2^2\xi & -a_1a_2\xi & -a_1a_2\eta & a_1^2\eta\\ -a_2b_2\xi & a_1b_2\xi & a_2b_1\eta & -a_1b_1\eta\\ -a_2b_2\xi & a_2b_1\xi & a_1b_2\eta & -a_1b_1\eta \end{bmatrix} \tag{69}$$

The above matrix can be obtained by using the following form for the enhanced displacement gradient $\mathbf{H}^{enh}$:

$$\mathbf{F}^{enh} = \mathbf{H}^{enh} = \frac{J_0}{J} \mathbf{J}_0^{-1} \tilde{\mathbf{H}} \mathbf{J}_0^{-T} \tag{70}$$

where the Jacobian at the element origin is given by

$$\mathbf{J}_0 = \begin{bmatrix} a_1 & b_1 \\ a_2 & b_2 \end{bmatrix} \tag{71}$$

and $\tilde{\mathbf{H}}$ is chosen as

$$\underline{\tilde{\mathbf{H}}} = \begin{bmatrix} \lambda_1 \xi & \lambda_2 \xi \\ \lambda_3 \eta & \lambda_4 \eta \end{bmatrix} \tag{72}$$

Recently instabilities have been detected in a non-linear version of the QM6 element. The QM6 element proposed by Taylor/Beresford/Wilson in 1976 can be viewed as an enhanced strain element with four enhanced strain terms. A non-linear version was proposed by Simo and Armero [8]. The non-physical instabilities in enhanced strain finite element simulations can occur in a hyperelastic material under uniform compression, as initially observed by Wriggers and Reese [20]. The problem has been investigated recently by several researchers, e.g. Crisfield et al. [11], de Souza Neto et al. [19], Glaser and Armero [13, 14].

In order to overcome the element instability problems, Glaser and Armero [13] proposed to exchange the original basis for the enhanced deformation gradient

$$\underline{\tilde{\mathbf{H}}} = \begin{bmatrix} \lambda_1 \xi & \lambda_2 \eta \\ \lambda_3 \xi & \lambda_4 \eta \end{bmatrix} \tag{73}$$

by either expression (72) or by

$$\underline{\tilde{\mathbf{H}}} = \begin{bmatrix} \lambda_1 \xi & \lambda_2 \xi + \lambda_3 \eta \\ \lambda_2 \xi + \lambda_3 \eta & \lambda_4 \eta \end{bmatrix} \tag{74}$$

Glaser and Armero considered the following two transformations for constructing the enhanced part of the deformation gradient:

$$\text{a)} \quad \mathbf{H}^{enh} = \frac{J_0}{J} \mathbf{J}_0 \tilde{\mathbf{H}} \mathbf{J}_0^{-1} \tag{75}$$

$$\text{b)} \quad \mathbf{H}^{enh} = \frac{J_0}{J} \mathbf{J}_0^{-T} \tilde{\mathbf{H}} \mathbf{J}_0^{-1} \tag{76}$$

The enhanced deformation gradient in reference [13] is chosen in the form

$$\mathbf{F}^{enh} = \mathbf{F}_0 \mathbf{H}^{enh} \tag{77}$$

as proposed by Simo/Armero and Taylor [9]. Korelc and Wriggers [15] proposed an enhanced deformation gradient of the form

$$\mathbf{F}^{enh} = \mathbf{H}^{enh} = \frac{J_0}{J} \mathbf{J}_0^{-T} \tilde{\mathbf{H}} \mathbf{J}_0^{-1} \tag{78}$$

where $\tilde{\mathbf{H}}$ is the same as in equation (72). However, Glaser and Armero pointed out that the use of (78) yields a non-objective element. For the proposed element $\mathbf{H}^{enh}$ is chosen as in equation (70). Using (70) an objective element is obtained (see example 5.7).

After elimination of the strain parameters the assumed displacement gradient for an increment takes the form

$$\Delta g_u = \bar{\mathbf{B}}\,\Delta \mathbf{q} + \bar{\mathbf{B}}^{enh}\,\Delta \boldsymbol{\lambda} \tag{79}$$

where

$$\bar{\mathbf{B}} = \begin{bmatrix} \bar{N}^1_X & 0 & \bar{N}^2_X & 0 & \bar{N}^3_X & 0 & \bar{N}^4_X & 0 \\ 0 & \bar{N}^1_Y & 0 & \bar{N}^2_Y & 0 & \bar{N}^3_Y & 0 & \bar{N}^4_Y \\ \bar{N}^1_Y & \bar{N}^1_X & \bar{N}^2_Y & \bar{N}^2_X & \bar{N}^3_Y & \bar{N}^3_X & \bar{N}^4_Y & \bar{N}^4_X \end{bmatrix} \tag{80}$$

and

$$\bar{\mathbf{B}}^{enh} = \begin{bmatrix} \bar{b}^{enh}_{11} & \bar{b}^{enh}_{12} & \bar{b}^{enh}_{13} & \bar{b}^{enh}_{14} \\ \bar{b}^{enh}_{21} & \bar{b}^{enh}_{22} & \bar{b}^{enh}_{23} & \bar{b}^{enh}_{24} \\ \bar{b}^{enh}_{31} & \bar{b}^{enh}_{32} & \bar{b}^{enh}_{33} & \bar{b}^{enh}_{34} \\ \bar{b}^{enh}_{41} & \bar{b}^{enh}_{42} & \bar{b}^{enh}_{43} & \bar{b}^{enh}_{44} \end{bmatrix} \tag{81}$$

The functions $\bar{b}^{enh}_{ij}(\xi,\eta)$ are defined as

$$\bar{b}^{enh}_{ij}(\xi,\eta) = \frac{L^1_{ij}}{\hat{h}_{11}} + \frac{L^2_{ij}}{\hat{h}_{22}}\,S_2(\xi,\eta) + \frac{L^3_{ij}}{\hat{h}_{33}}\,S_3(\xi,\eta) \tag{82}$$

and

$$L^k_{ij} = \int_V S_k(\xi,\eta) b^{enh}_{ij}(\xi,\eta)\,dV. \tag{83}$$

The functions b^{enh}_{ij} are the coefficients of the matrix $\mathbf{B}^{enh}$ defined with equation (69).

Because the assumed displacement gradient can be expressed in the form (79) involving the sparse matrix $\bar{\mathbf{B}}$, the element tangent stiffness matrix can be computed in a very economic manner: The element tangent stiffness matrix for the large deformation case is given as

$$\mathbf{k}_T = \mathbf{K}_T - \boldsymbol{\Gamma}_T^T \mathbf{Q}_T^{-1} \boldsymbol{\Gamma}_T \tag{84}$$

where the matrices $\mathbf{K}_T$, $\boldsymbol{\Gamma}_T$, and $\mathbf{Q}_T$ can be computed in the following form:

$$\begin{aligned} \mathbf{K}_T &= = \int_V \bar{\mathbf{B}}^T \mathbf{A}_T \bar{\mathbf{B}}\,dV \\ \boldsymbol{\Gamma}_T &= = \int_V \bar{\mathbf{B}}^{enh\,T} \mathbf{A}_T \bar{\mathbf{B}}\,dV \\ \mathbf{Q}_T &= = \int_V \bar{\mathbf{B}}^{enh\,T} \mathbf{A}_T \bar{\mathbf{B}}^{enh}\,dV \end{aligned} \tag{85}$$

The residual vectors for step n are obtained by computing

$$\mathbf{f}_{int} = = \int_V \bar{\mathbf{B}}^T \mathbf{P}_n \, dV , \qquad \mathbf{f}_{int}^{enh} = = \int_V \bar{\mathbf{B}}^{enh\,T} \mathbf{P}_n \, dV \tag{86}$$

4. Chosen Constitutive Models

For the examples in the present paper we consider two constitutive models.

4.1 Model 1

The stored energy function for the first constitutive model is

$$W = W(I_1, I_2, I_3) = \hat{W}(I_1, J) = \frac{1}{2}\mu(I_1 - 3) - \mu \ln J + \frac{1}{2}\lambda(\ln J)^2 \tag{87}$$

where I_1, I_2, I_3 are the invariants of the right Cauchy-Green deformation tensor

$$\mathbf{C} = \mathbf{F}^T\mathbf{F} \tag{88}$$

and

$$J = \sqrt{I_3} = \sqrt{\det \mathbf{C}} = \det \mathbf{F} \tag{89}$$

The second Piola-Kirchhoff stress tensor is obtained from

$$\mathbf{S} = 2\frac{\partial W}{\partial \mathbf{C}} = 2\frac{\partial W}{\partial I_1}\frac{\partial I_1}{\partial \mathbf{C}} + 2\frac{\partial W}{\partial I_2}\frac{\partial I_2}{\partial \mathbf{C}} + 2\frac{\partial W}{\partial I_3}\frac{\partial I_3}{\partial \mathbf{C}} \tag{90}$$

where

$$\frac{\partial I_1}{\partial \mathbf{C}} = \mathbf{I}$$

$$\frac{\partial I_3}{\partial \mathbf{C}} = (\det \mathbf{C})\mathbf{C}^{-1} = J^2\mathbf{C}^{-1} = J^2\mathbf{F}^{-1}\mathbf{F}^{-T} \tag{91}$$

For the above strain energy function W we have

$$\frac{\partial W}{\partial I_1} = \frac{1}{2}\mu$$

$$\frac{\partial W}{\partial I_2} = 0 \tag{92}$$

$$\frac{\partial W}{\partial I_3} = \frac{\partial W}{\partial J}\frac{\partial J}{\partial I_3} = \frac{\partial W}{\partial J}\frac{1}{2J}$$

and

$$\frac{\partial W}{\partial J} = \frac{\mu}{J} + \lambda\frac{1}{J}\ln J \tag{93}$$

so that we get the constitutive relationship for S in the form

$$\mathbf{S} = \mu\mathbf{I} + [-\mu + \lambda \ln J]\mathbf{F}^{-1}\mathbf{F}^{-T} \tag{94}$$

For the other stresses we obtain

$$\mathbf{P} = \mu[\mathbf{F} - \mathbf{F}^{-T}] + \lambda \ln J\, \mathbf{F}^{-T}$$

$$\tau = \mu[\mathbf{b} - \mathbf{I}] + \lambda \ln J\, \mathbf{I} \tag{89}$$

$$\sigma = \frac{\mu}{J}[\mathbf{b} - \mathbf{I}] + \frac{\lambda}{J} \ln J\, \mathbf{I}$$

where

$$\mathbf{b} = \mathbf{F}\mathbf{F}^{T} \tag{96}$$

The first elasticity tensor $\mathbf{A}$ can be obtained conveniently by using components of the un-symmetric Piola-Kirchhoff stress tensor $\mathbf{P}$, given from (56) by

$$P_{11} = \mu F_{11} + \frac{1}{J}[-\mu + \lambda \ln J]F_{22}\,, \qquad P_{22} = \mu F_{22} + \frac{1}{J}[-\mu + \lambda \ln J]F_{11}$$

$$P_{12} = \mu F_{12} - \frac{1}{J}[-\mu + \lambda \ln J]F_{21}\,, \qquad P_{21} = \mu F_{21} - \frac{1}{J}[-\mu + \lambda \ln J]F_{12} \tag{97}$$

Using relationship (59) we get

$$A_{1111} = \mu + \frac{1}{J^2}[\mu + \lambda - \lambda \ln J]F_{22}F_{22}\,, \qquad A_{2222} = \mu + \frac{1}{J^2}[\mu + \lambda - \lambda \ln J]F_{11}F_{11}$$

$$A_{1122} = \frac{1}{J}[-\mu + \lambda \ln J] + \frac{1}{J^2}[\mu + \lambda - \lambda \ln J]F_{22}F_{11}$$

$$A_{1112} = -\frac{1}{J^2}[\mu + \lambda - \lambda \ln J]F_{22}F_{21}\,, \qquad A_{1121} = -\frac{1}{J^2}[\mu + \lambda - \lambda \ln J]F_{22}F_{12}$$

$$A_{2212} = -\frac{1}{J^2}[\mu + \lambda - \lambda \ln J]F_{11}F_{21}\,, \qquad A_{2221} = -\frac{1}{J_2}[\mu + \lambda - \lambda \ln J]F_{11}F_{12} \tag{98}$$

$$A_{1212} = \mu + \frac{1}{J^2}[\mu + \lambda - \lambda \ln J]F_{21}F_{21}\,, \qquad A_{2121} = \mu + \frac{1}{J^2}[\mu + \lambda - \lambda \ln J]F_{12}F_{12}$$

$$A_{1221} = -\frac{1}{J}[-\mu + \lambda \ln J] + \frac{1}{J^2}[\mu + \lambda - \lambda \ln J]F_{21}F_{12}$$

In matrix notation the incremental constitutive equation for a point under consideration can be written as

$$\Delta\mathbf{P} = \mathbf{A}_{\mathbf{T}}\, \Delta\mathbf{F} \tag{99}$$

where

$$\mathbf{A}_{\mathbf{T}} = \begin{bmatrix} A_{1111} & A_{1122} & A_{1112} & A_{1121} \\ A_{2211} & A_{2222} & A_{2212} & A_{2221} \\ A_{1211} & A_{1222} & A_{1212} & A_{1221} \\ A_{2111} & A_{2122} & A_{2112} & A_{2121} \end{bmatrix}$$

$$\Delta\mathbf{P}^{T} = [P_{11},\ P_{22},\ P_{12},\ P_{21}] \tag{100}$$

$$\Delta\mathbf{F}^{T} = \nabla(\Delta\mathbf{u}^{T}) = [\Delta u_X,\ \Delta v_Y,\ \Delta u_Y,\ \Delta v_X]$$

4.2 Model 2

The second constitutive model used in the examples is taken from a paper by Knowles and Sternberg [29]. The strain energy function for this model is

$$W(I_1, J) = \frac{1}{2}\mu[I_1 J^{-2} + 2J - 4] \tag{101}$$

Reference [29] gives a detailed discussion of this material model which is a special case of a Blatz-Ko material.

5. Numerical examples

Several linear and nonlinear problems have been selected to test the performance of the proposed four-node element denoted as $\bar{B}$–QE4. For all problems 2x2 Gaussian integration is used. The element passes the patch test.

5.1 Beam bending

A beam modeled with five elements is subjected to two load cases (Figure 1). Plane stress conditions are assumed in the model. The results of different elements for the maximum displacement at point A and the normal stress σ_{xx} at point B are given in Table 1. The elements used in the examples are: i) the bilinear isoparametric displacement element Q4 [30,31,32], ii) the enhanced strain element QM6 of Taylor/Beresford/Wilson [4], iii) the hybrid stress element P-S of Pian/Sumihara [6], iv) the enhanced mixed element QE2 by Piltner/Taylor [1], v) the proposed element $\bar{B}$-QE4. The elements $\bar{B}$-QE4 and QE2 give identical results.

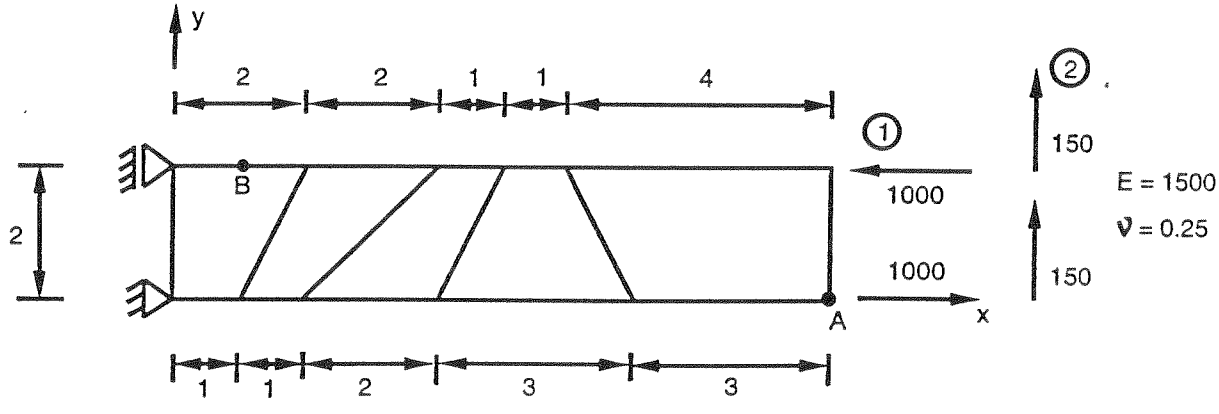

Figure 1: Finite element mesh for cantilever beam problem

Table 1: Comparison of plane stress solutions obtained with four node elements for cantilever beam problems.

	Case 1		Case 2	
element	v_A	σ_{xxB}	v_A	σ_{xxB}
Q4	45.49	-1604	50.80	-2146
QM6	96.07	-2497	97.98	-3235
P-S	96.18	-3001	98.05	-3899
QE2	96.5	-3004	98.26	-3906
$\bar{B}$-QE4	96.5	-3004	98.26	-3906
exact	100	-3000	102.6	-4050

5.2 Mesh distortion test for beam bending

In this test a beam under bending is analyzed with only two plane stress elements (Figure 2). The degree of distortion of the element is measured with the distortion parameter Δ. The material parameters are $E = 1500$ and $\nu = 0.25$. From Table 2 we can see that the elements QE2 and $\bar{B}$-QE4 show the least sensitivity to mesh distortion even for very severe distortions. Elements QE2 and $\bar{B}$-QE4 provide identical results.

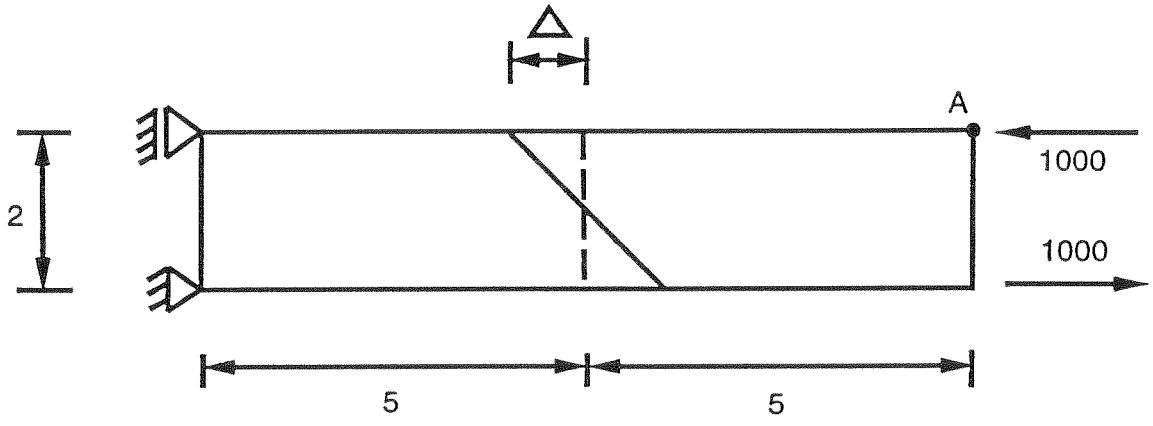

Figure 2: Cantilever beam for the mesh distortion test

Table 2: Displacement v_A of cantilever beam (Figure 2) for different values of the mesh distortion parameter Δ

displacement v_A						
Δ	Q4	QM6	P-S	QE2	$\bar{B}$-QE4	Exact
0	28.0	100.0	100.0	100.0	100.0	100
0.5	21.0	80.9	81.0	81.2	81.2	100
1	14.1	62.7	62.9	63.4	63.4	100
2	9.7	54.4	55.0	56.5	56.5	100
3	8.3	53.6	54.7	57.5	57.5	100
4	7.2	51.2	53.1	57.9	57.9	100
4.9	6.2	46.8	49.8	56.9	56.9	100

5.3 Cook's membrane problem

The material parameters for the plane stress structure shown in Figure 3 are $E = 1$ and $\nu = 1/3$. Displacement and stress results are listed in Table 3.

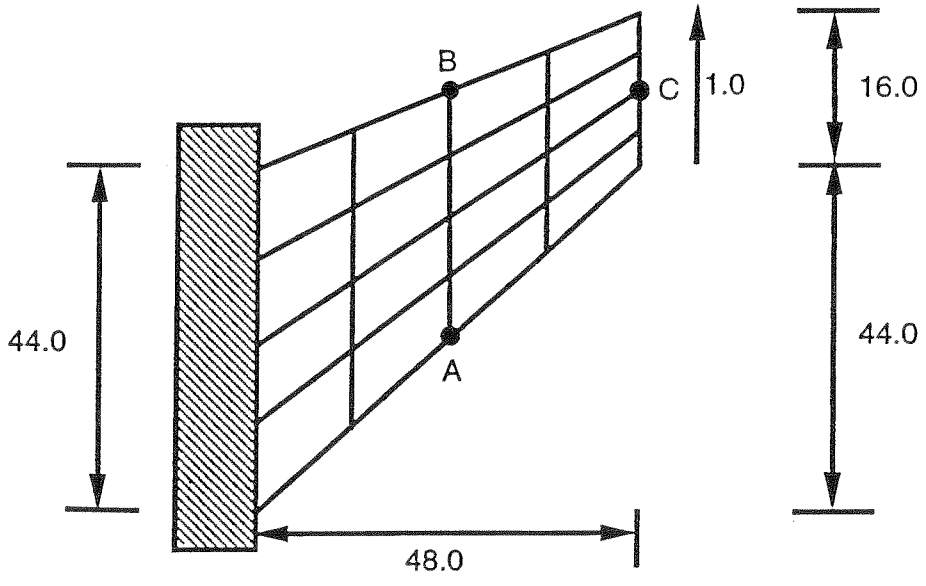

Figure 3: Cook's membrane problem: plane stress structure with unit load uniformly distributed along right edge ($E = 1$, $\nu = 1/3$).

Table 3: Results for the problem shown in Figure 3.

displacement v at C			
element	N=2	N=4	N=16
Q4	11.85	18.30	23.43
QM6	21.05	23.02	23.88
P-S	21.13	23.02	23.88
QE2	21.35	23.04	23.88
$\bar{B}$-QE4	21.35	23.04	23.88

maximum stress at A			
element	N=2	N=4	N=16
Q4	0.1078	0.1814	0.2353
QM6	0.1773	0.2225	0.2364
P-S	0.1854	0.2241	0.2364
QE2	0.1956	0.2261	0.2364
$\bar{B}$-QE4	0.1956	0.2261	0.2364

5.4 Short beam under bending

A short beam, supported at the left end and subjected to a couple at the right edge, is modeled with a mesh as shown in Figure 4. The purpose of this example is to test the influence of the mesh pattern on the stress distribution in the finite element solution. In the QM6 element the stress has the tendency to line up with the element edges of the element in the center of the mesh (Figure 5a). On the other hand elements QE2 and $\bar{B}$-QE4 preserve symmetries in the solution domain although a very coarse irregular mesh is used (Figure 5b).

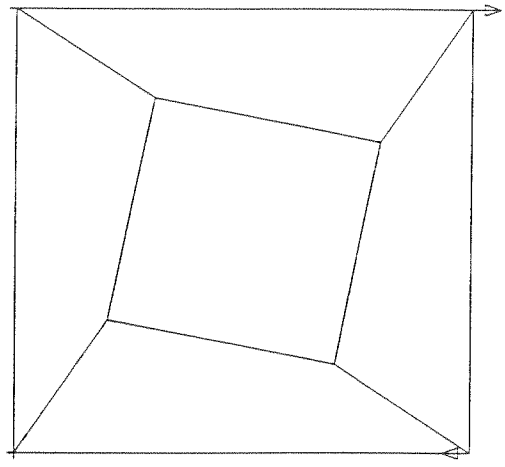

Figure 4: Finite element mesh for a short beam under bending

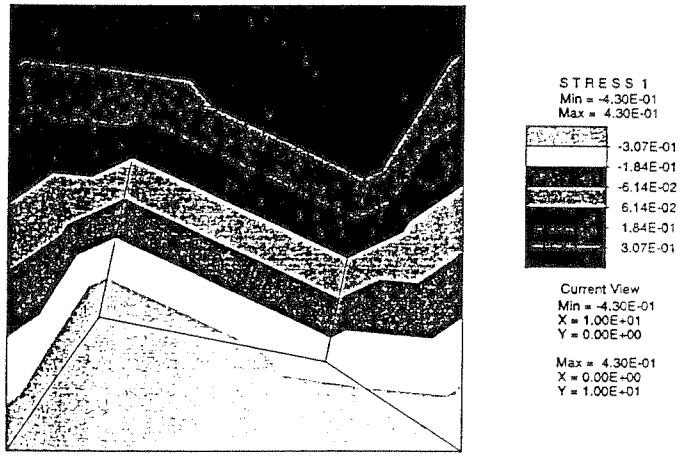

Figure 5a: Stress σ_{xx} obtained with element QM6

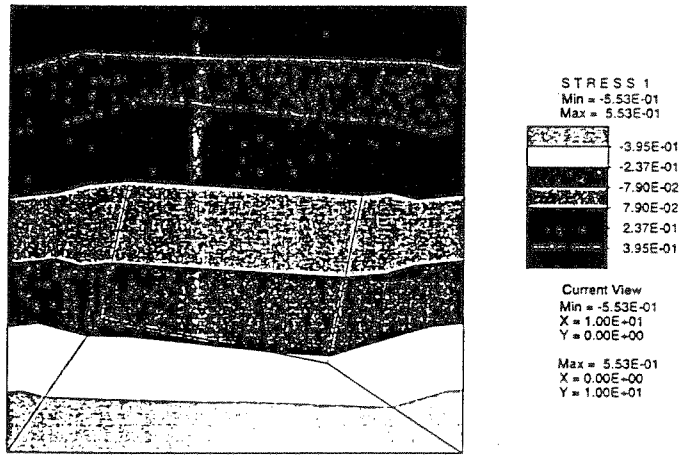

Figure 5b: Stress σ_{xx} obtained with elements QE2 and $\bar{B}$-QE4

5.5 Single element test for a Neo-Hookean material model

Wriggers and Reese [20] noticed that the enhanced element Q1/E4 [8] can experience problems in the analysis of Neo-Hookean hyperelastic materials under uniform compression. They suggested the single element test shown in Figure 6. The material model (87) is used with the following material parameters: $\lambda = 40000$, $\mu = 80.2$. At 30.4% compression the element Q1/E4 yields a non-physical instability. The element tangent matrix has two negative eigenvalues at this deformation level, whereas the system tangent matrix has one negative eigenvalue. However, the element tangent matrix should have only one negative eigenvalue for this deformation. On the other hand the element $\bar{B}$-QE4 keeps only one negative eigenvalue for the element tangent matrix, up to almost 100% compression.

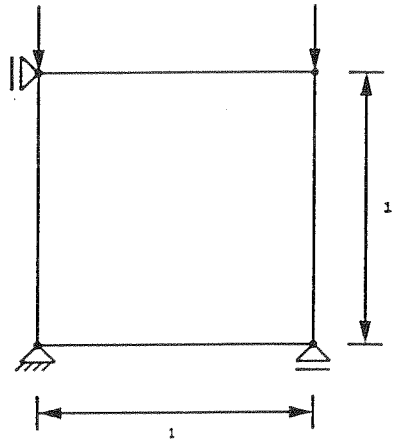

Figure 6: Finite element under compression

5.6 Multi-element test for a Neo-Hookean material model

One half of a block with unit sides is discretized with a 10 x 20 element mesh. The material parameters for the Neo-Hookean model are chosen as in example 5.5. The element Q1/E4 yields a non-physical instability at 30.4%. However, the first physical instability should appear at 49.6% compression. The element $\bar{B}$-QE4 is able to detect this physical instability.

5.7 Objectivity test for large deformation

The beam shown in Figure 7a is fixed at the right end and subjected to a prescribed displacement as illustrated in Figure 7b. After calculating the displacements and stresses the structure is rotated and displacements and stresses are calculated for each rotation angle ($\theta = 10°, 20°, ..., 180°$). For the $\bar{B}$-QE4 element the results are independent of the rotation angle. It should be noticed that the results are not frame independent if we use enhanced strains based on equation (76) instead of (70).

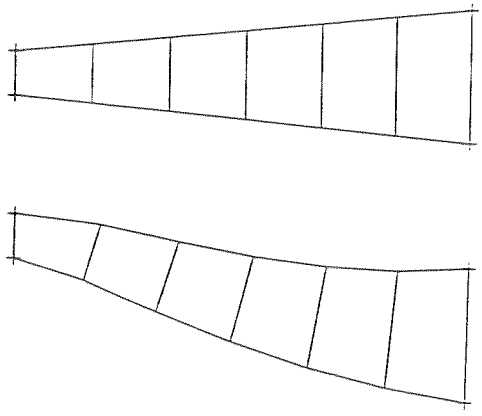

Figure 7: a) undeformed beam; b) deformed beam and FE mesh

5.8 Material 2 subjected to a homogeneous plane deformation

One half of a block of dimensions 1 x 1 is dicretized with non-rectangular elements (Figure 8). The block is subjected to plane strain uni-axial stress parallel to the x_1-axis. Material model 2 is used with $\mu = 100$. The analytical solution for σ_1 in this problem is given as a function of the stretch λ_1 (Figure 9):

$$\sigma_1 = 100(1 - \lambda_1^{-8/3}) \tag{102}$$

For every element in the mesh stresses can be calculated exactly.

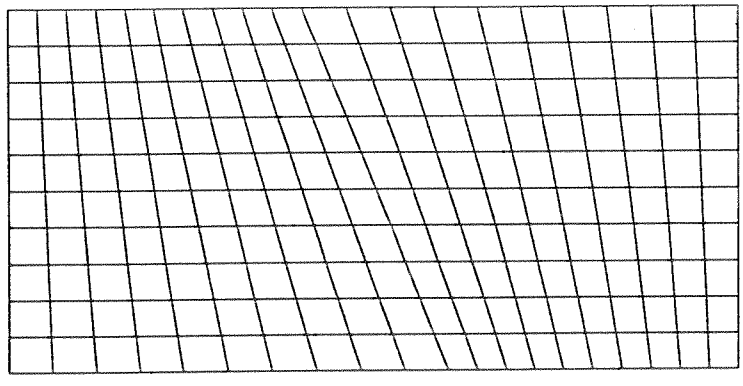

Figure 8: Finite element discretization for example 5.8

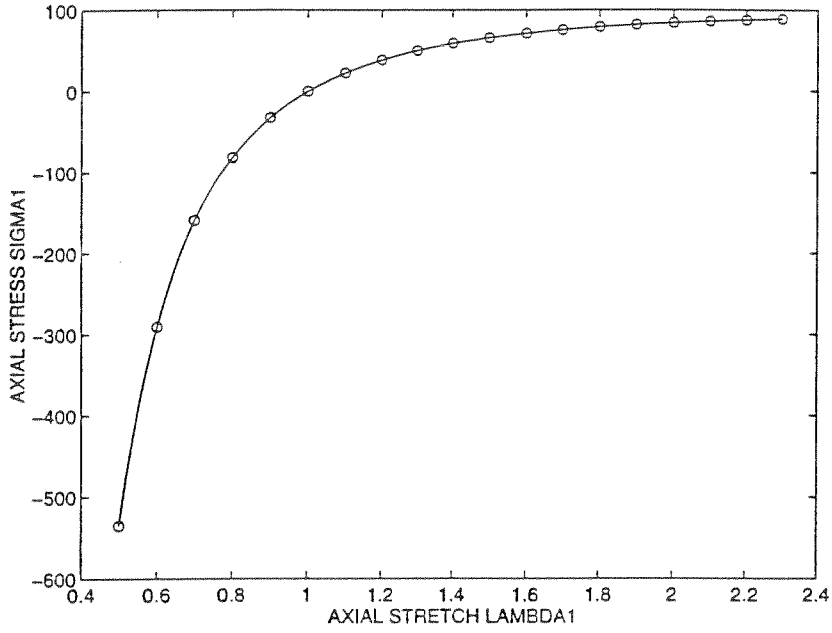

Figure 9: Material 2. Cauchy stress vs. axial stretch

In Figure 9, the solid line represents the analytical solution and the circles stand for stress values obtained numerically for a chosen finite element in the mesh.

6 Concluding remarks

For linear problems, elements $\overline{B}$-QE4 and QE2 give identical results and show an overall very good behavior. The advantage of element $\overline{B}$-QE4 is that it can be coded very similar to a displacement element and therefore runs faster than element QE2. The key for a fast linear and non-linear element implementation is to use orthogonal stress and strain functions in the mixed variational formulation. Due to the use of orthogonal functions matrix inversions for strain and stress parameters at the element level can be avoided in a finite element program. In the current implementation standard shape function derivatives N_x, N_y are exchanged by $\overline{N}_x$ and $\overline{N}_y$ functions derived in the paper. For non-linear problems the displacement like implementation of the mixed element $\overline{B}$-QE4 has the obvious advantage that it is time saving compared to an implementation of the mixed variational formulation with matrix inversions for strain and stress parameters.

REFERENCES

[1] R. Piltner and R.L. Taylor, "A quadrilateral finite element with two enhanced strain modes", Int. J. Numer. Meth. Eng., 38, 1783 - 1808, (1995).

[2] T.J.R. Hughes, "Equivalence of finite elements for nearly incompressible elasticity", J. Appl. Mech. 44, 181 - 183, (1977).

[3] T.J.R. Hughes, "Generalizing of selective integration procedures to anisotropic and nonlinear media", Int. J. Numer. Meth. Eng., 15, 1413 - 1418, (1980).

[4] R.L. Taylor, P.J. Beresford and E.L. Wilson, "A non-conforming element for stress analysis", Int. J. Numer. Meth. Eng., 10, 1211 - 1219, (1976).

[5] J.C. Simo and M.S. Rifai, "A class of mixed assumed strain methods and the method of incompatible modes", Int. J. Numer. Meth. Eng., 29, 1595 - 1638, (1990).

[6] T.H.H. Pian and K. Sumihara, "Rational approach for assumed stress elements", Int. J. Numer. Meth. Eng., 20, 1685 - 1695, (1984).

[7] K.-Y. Yuan, Y.-S. Huang and T.H.H. Pian, "New strategy for assumed stresses for 4-node hybrid stress membrane element", Int. J. Numer. Meth. Eng., 36, 1747 - 1763, (1993).

[8] J.C. Simo and F. Armero, "Geometrically non-linear enhanced strain mixed methods and the method of incompatible modes", Int. J. Numer. Meth. Eng., 33, 1413 - 1449, (1992).

[9] J.C. Simo, F. Armero and R. L. Taylor, "Improved versions of assumed enhanced strain tri-linear elements for 3D finite deformation problems", Comput. Methods Appl. Mech. Engrg. 110, 359 - 386, (1993).

[10] U. Andelfinger and E. Ramm, "EAS-elements for two-dimensional, three-dimensional, plate and shell structures and their equivalence to HR-elements", Int. J. Numer. Meth. Eng., 36, 1311 - 1337, (1993).

[11] M. A. Crisfield, G.F. Moita, G. Jelenic and L.P.R. Lyons, "Enhanced lower-order element formulations for large strains", pp. 293 - 320, in: Computational Plasticity - Fundamentals and Applications, ed. by D.R.J. Owen and E. Onate, Pineridge Press, Swansea, 1995.

[12] C. Freischläger and K. Schweizerhof, "On a systematic development of trilinear three-dimensional solid elements based on Simo's enhanced strain formulation", International Journal of Solids and Structures, 33, 2993-3017, (1996).

[13] S. Glaser and F. Armero, "Recent developments in the formulation of assumed enhanced strain finite elements for finite deformation problems", Report No. UCB/SEMM-95/13, University of California, Berkeley, 1995.

[14] S. Glaser and F. Armero, "On the formulation of Enhanced Strain Finite Elements in Finite Deformations", submitted to Engineering Computations, 1996.

[15] J. Korelc and P. Wriggers, "Consistent gradient formulation for a stable enhanced strain method for large deformations", Engineering Computations, 13, 103 - 123, (1996).

[16] P. Wriggers and J. Korelc, "On enhanced strain methods for small and finite deformations of solids", Computational Mechanics, 18, 413 - 428, (1996).

[17] J.C. Nagtegaal and D.D Fox, "Using assumed enhanced strain elements for large compressive deformation", International Journal of Solids and Structures, 33, 3151-3159, (1996).

[18] D. Roehl and E. Ramm, "Large elasto-plastic finite element analysis of solids and shells with the enhanced assumed strain concept", International Journal of Solids and Structures, 33, 3215-3237, (1996).

[19] E.A. de Souza Neto, D. Peric, G.C. Huang and D.R.J. Owen, "Remarks on the stability of enhanced strain elements in finite elasticity and elastplasticity", pp. 361 - 372, in: Computational Plasticity - Fundamentals and Applications, ed. by D.R.J. Owen and E. Onate, Pineridge Press, Swansea, 1995.

[20] P. Wriggers and S. Reese, "A note on enhanced strain methods for large deformations", Comput. Methods Appl. Mech. Engrg. 135, 201 - 209, (1996).

[21] J. Jirousek, and L. Guex, "The hybrid-Trefftz finite element model and its application to plate bending", Int. J. Numer. Methods Eng., 23, 651 - 693, (1986).

[22] J. Jirousek, "Hybrid-Trefftz plate bending elements with p-method capabilities", Int. J. Num. Methods Eng., 24, 1367 - 1393 (1987)

[23] J. Jirousek, A. Venkatesh, A.P. Zielinski and H. Rabemanantsoa, "Comparative study of p-extensions based on conventional assumed displacement and hybrid-Trefftz FE models", Computers & Structures, 46, 261 - 278, (1993).

[24] Piltner, R.: Recent developments in the Trefftz method for finite element and boundary element applications, Advances in Engineering Software 24, 107 - 115, (1995).

[25] R. Piltner, "A quadrilateral hybrid-Trefftz plate bending element for the inclusion of warping based on a three-dimensional plate formulation", Int. J. Num. Methods Eng., 33, 387 - 408 (1992)

[26] Zielinski, A.P. and Zienkiewicz, O.C.: Generalized finite element analysis with T-complete solution functions. Int. J. Num. Methods Eng., 21, 509 - 528, (1985).

[27] M.F. Beatty, "Introduction to Nonlinear Elasticity", pp. 13 - 112, in: Nonlinear Effects in Fluids and Solids, Eds.: M.M. Carroll and M.A. Hayes, Plenum Press, New York/London, 1996.

[28] M.F. Beatty, "Topics in Finite Elasticity: Hyperelasticity of Rubber, Elastomers, and Biological Tissues - with Examples", Applied Mechanics Reviews, Vol. 40, pp. 1699 - 1734, 1987.

[29] J.K. Knowles and Eli Sternberg, "On the failure of ellipticity and the emergence of discontinuous deformation gradients in plane finite elastostatics", Journal of Elasticity, 8 (4), 329 - 379, (1978).

[30] I.C. Taig, "Structural analysis by the matrix displacement method", English Electric Aviation Report No. S017, 1961.

[31] T.J.R. Hughes, "The Finite Element Method", Prentice-Hall, Englewood Cliffs, N.J., 1987.

[32] K.-J. Bathe, E.L. Wilson, "Numerical Methods in Finite Element Analysis", Prentice-Hall, Englewood Cliffs, New Jersey, 1976.